SLAC-PUB-13955

Strong energy-momentum dispersion of phonon-dressed carriers in the lightly doped band insulator $SrTiO_3$

W. Meevasana[1,2], X. J. Zhou[3], B. Moritz[2], C-C. Chen[1,2], R.H. He[1,2], S.-I. Fujimori[4], D.H. Lu[2], S.-K. Mo[1,5], R.G. Moore[2], F. Baumberger[6], T.P. Devereaux[2], D. van der Marel[7], N. Nagaosa[8,9], J. Zaanen[10], Z.-X. Shen[1,2]

[1]Departments of Physics and Applied Physics, Stanford University, CA 94305, USA
[2]Stanford Institute for Materials and Energy Sciences, SLAC National Accelerator Laboratory, 2575 Sand Hill Road, Menlo Park, CA 94025, USA
[3]Institute of Physics, Chinese Academy of Sciences, Beijing 100190, China
[4]Synchrotron Radiation Research Unit, Japan Atomic Energy Agency, Mikazuki, Hyogo 679-5148, Japan
[5]Advanced Light Source, Lawrence Berkeley National Lab, Berkeley, CA 94720, USA
[6]School of Physics and Astronomy, University of St Andrews, North Haugh, St. Andrews, Fife KY16 9SS, UK
[7]Département de Physique de la Matière Condensée, Université de Genève, quai Ernest-Ansermet 24, CH1211 , Genève 4, Switzerland
[8]Department of Applied Physics, The University of Tokyo, Bunkyo-ku, Tokyo 1138656, Japan
[9]Cross-Correlated Materials Research Group (CMRG), ASI, RIKEN, Wako 351-0198, Japan
[10]The Instituut-Lorentz for Therorectical Physics, Leiden University, Leiden, The Netherlands

Abstract. Much progress has been made recently in the study of the effects of electron-phonon (el-ph) coupling in doped insulators using angle resolved photoemission (ARPES), yielding evidence for the dominant role of el-ph interactions in underdoped cuprates. As these studies have been limited to doped Mott insulators, the important question arises how this compares with doped band insulators where similar el-ph couplings should be at work. The archetypical case is the perovskite $SrTiO_3$ (STO), well known for its giant dielectric constant of 10000 at low temperature, exceeding that of La_2CuO_4 by a factor of 500. Based on this fact, it has been suggested that doped STO should be the archetypical bipolaron superconductor. Here we report an ARPES study from high-quality surfaces of lightly doped $SrTiO_3$. Comparing to lightly doped Mott insulators, we find the signatures of only moderate electron-phonon coupling: a dispersion anomaly associated with the low frequency optical phonon with a $\lambda' \sim 0.3$ and an overall bandwidth renormalization suggesting an overall $\lambda' \sim 0.7$ coming from the higher frequency phonons. Further, we find no clear signatures of the large pseudogap or small polaron phenomena. These findings demonstrate that a large dielectric constant itself is not a good indicator of el-ph coupling and highlight the unusually strong effects of the el-ph coupling in doped Mott insulators.

Work supported in part by US Department of Energy contract DE-AC02-76SF00515.

PACS numbers: 71.38.-k, 71.18.+y, 71.20.-b, 71.27.+a

Submitted to: *New J. Phys.*

1. Introduction

The notion that carriers doped into insulators get dressed by lattice deformations has been around for a long time[1, 2]. A recent development is that this polaron formation can be studied experimentally using ARPES yielding more direct information on the physics than classical transport and optical spectroscopic methods. Especially when the carrier density is small but finite, where a controlled theoretical framework is lacking, ARPES has been quite revealing. The case has been made that lightly doped cuprates fall victim to small polaron formation (strong interacting case) that is vulnerable to self trapping by impurities [3, 4]: in undoped cuprates the spectral functions reveal Frank-Condon type broad humps caused by the coupling to multiple phonons, and only when doping is increased, a well-defined quasi-particle (QP) peak starts to emerge [3, 4]. Another recent ARPES revelation is found in the context of highly doped manganites in the colossal magneto resistance regime. At high temperatures ARPES reveals the Frank-Condon humps signaling small polarons, while upon lowering temperature small pole-strength quasiparticle peaks appear in addition, indicating that a coherent Fermi-liquid is formed from the microscopic polarons[5].

Both manganites and cuprates are doped Mott-insulators and no modern ARPES information is available on polaron physics in the simpler doped band insulators. We therefore decided to focus on the classic $SrTiO_3$ doped band insulator. $SrTiO_3$ is known to have an exceptionally high static dielectric constant on the order of 10^4 at low temperature [6]. Superconductivity can be induced by electron doping with either O, Nb, or La[7, 8] over a narrow range of low carrier concentrations between $\sim 10^{19}$ to $\sim 10^{20}$ cm^{-3}. The optimal T_c is typically 0.2-0.3 K but can reach up to 1.2 K[9] which is surprisingly high for such low carrier concentrations. It has been speculated that this is due to the formation of bipolarons[10]. However, whether small polarons actually exist in $SrTiO_3$ depends on the relevant length scale for the electron-phonon couplings.

The case was made in a recent optical study by van Mechelen *et al.* that the electron-phonon coupling is actually not that strong at all[11]. ARPES is however more direct in revealing the strength of the coupling to specific phonons. With this technique we arrive at the verdict that doped STO has no dealings with small polarons and that the electron-phonon coupling acts in a perturbative way.

2. Methods and Materials

The samples investigated here are $La_xSr_{1-x}TiO_{3+\delta}$ (Crystal Base Co., Japan) at nominal dopings of $x = 0.01$ ($T_c \sim 0.2$ K) and $x = 0.05$ (non superconducting) [8] while the actual doping levels at the surface are slightly different due to oxygen vacancies. We obtain high-quality surfaces by cleaving along guiding lines at T = 10 K and measure at the same temperature. This new technique results in significantly flatter surfaces than fracturing or scraping of $SrTiO_3$. This was found to substantially improve the quality of ARPES data and enable us to see a clear quasi-particle band dispersion and dispersion

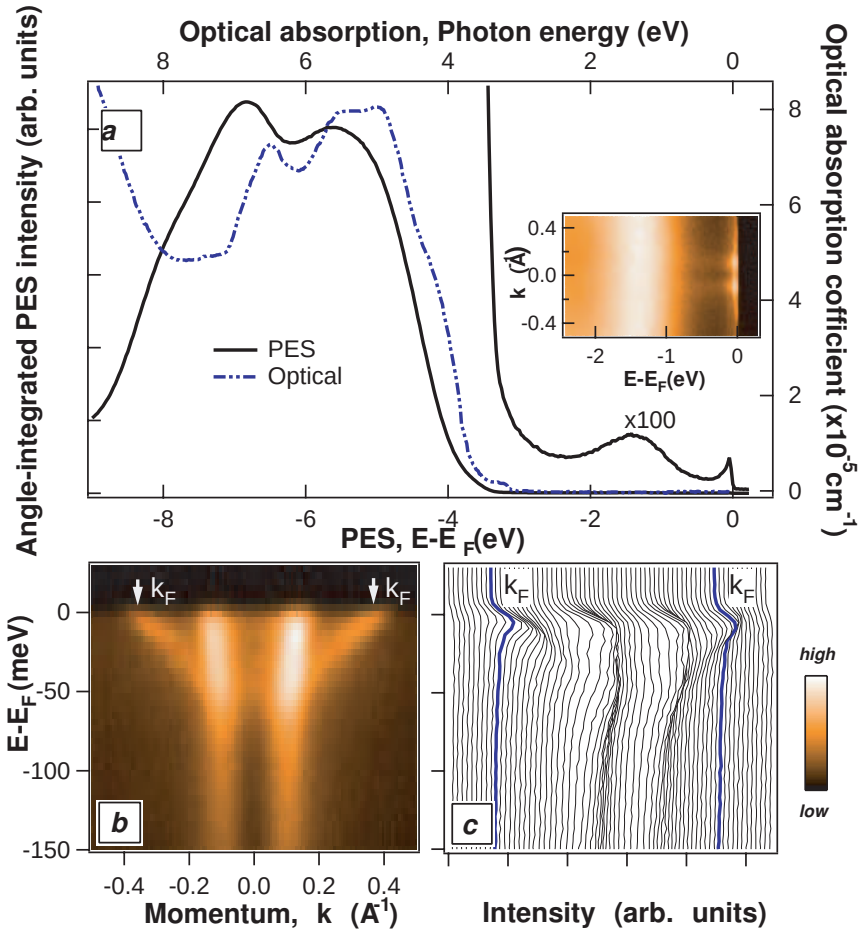

Figure 1. ARPES data of $x = 0.01$ sample at $T = 10$K. (a) Angle-integrated photoemission spectrum up to 9 eV in binding energy, together with optical absorption data of an undoped sample from Ref. [15]. The inset shows angle-resolved data of the in-gap state around 1.3 eV. (b) Quasi-particle band dispersion in the (010) plane near E_F (see cut b in Fig. 2(f)) with corresponding energy distribution curves in (c).

anomaly which have not been seen in previous measurements[12, 13, 14]

ARPES data were collected on a Scienta-4000 analyzer at the Stanford Synchrotron Radiation Laboratory (SSRL), Beamline 5-4, and the Advanced Light Source (ALS), Beamline 10.0.1, with photon energies between 18-90 eV and a base pressure of $< 4\times10^{-11}$ torr. Samples were cleaved *in situ* along the (001) plane at the measurement temperature, T = 10 K. A sharp (1×1) low-energy-electron-diffraction pattern indicates a well-ordered surface devoid of any reconstructions. The energy resolution was set to 9-11 meV and 15-20 meV for 18-35 eV and 35-90 eV photon energies respectively and the angular resolution was 0.35°. Additionally, a LSCO sample with x=0.01 was measured at ALS with photon energy = 55eV and T = 20K.

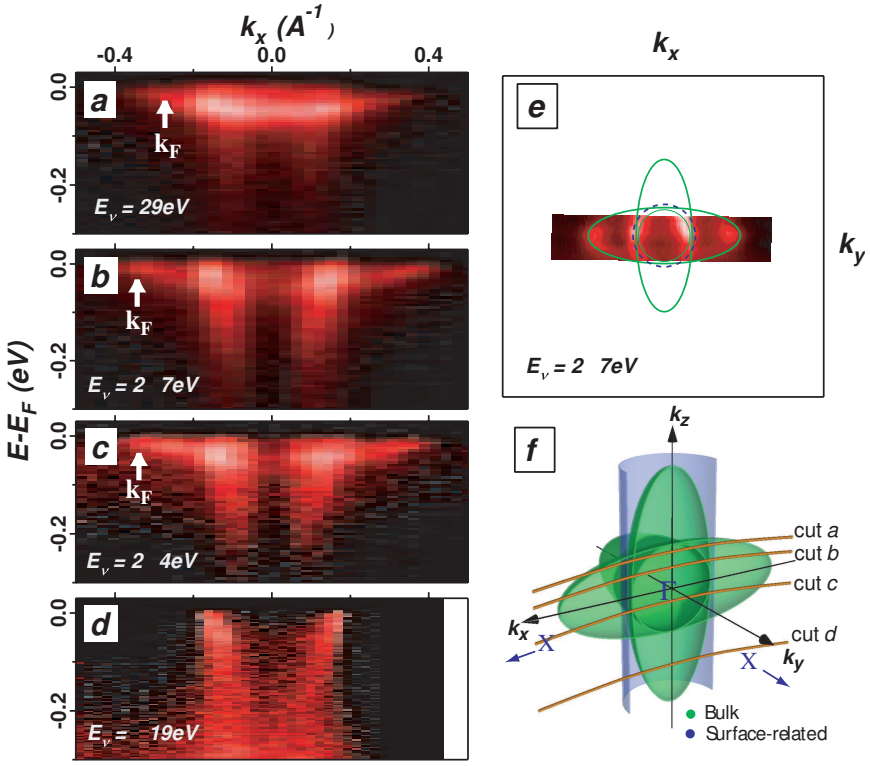

Figure 2. Fermi surface topography of $SrTiO_3$. (a) - (d) Band dispersion in the (010) plane for photon energies of 19, 24, 27 and 29 eV, respectively. Doped $SrTiO_3$ has a cubic unit cell and a three-dimensional Fermi surface, consisting of three ellipsoid-like surfaces along each axis (see more detail in Ref. [14]); when including the spin orbit coupling term in calculation [11], a shift in the Fermi surface occurs as shown in Fig. 3(e). (e) Fermi surface map near the Brillouin zone mid-plane ($h\nu$ =27eV). The solid green lines are guides to the eye. Estimated k_z positions for (a)-(d) are indicated by the orange lines in the schematic Fermi surface (f), where half of the whole Fermi surface is plotted; green (blue) indicates bulk (surface) band. Note that in $x = 0.01$ samples a second bulk band is expected with a Fermi crossing near the surface band. However, this band appears to be overshadowed by the more intense surface related band and further suppressed by the matrix element near Γ point.

3. Results

In Fig. 1, we present ARPES data taken at a photon energy of 27 eV. The dominant features in the angle integrated spectrum are the valence band between 3.3 eV and 9 eV, an in-gap state near 1.3 eV and the QP peak at the Fermi level. The energy gap between the onset of the oxygen valence bands to the QP band bottom is around 3.3 eV consistent with optical measurements[15] while local-density-approximation (LDA) band structure calculations predict a gap of $\sim$ 2 eV[14, 16]. The presence of a non-dispersive and broad in-gap state around 1.3 eV has been discussed in the literature (Ref. [13] and refs. therein) as caused by a local screening effect, chemical disorder or

donor levels.

Having established the basic spectral features, we now focus on the Fermi surface topography of $SrTiO_3$. Fig. 2(a)-2(d) show ARPES data taken at various photon energies (changing k_z) together with a Fermi surface map at 27 eV, projected on the k_x-k_y plane (Fig. 2(e)). The flatter band with a ∼60 meV band bottom (i.e. in Fig. 2(a)-2(c)) corresponds to a bulk state since the k_F crossing changes with different photon energy (changing k_z), in agreement with LDA calculations by I.I. Mazin where the computational details are the same as in Ref. [11]. The steeper band with a bottom ∼200 meV (e.g. in Fig. 2(d)) can be attributed to the surface of cleaved $SrTiO_3$ because the data do not show noticeable dispersion along k_z and they are absent in LDA calculations (indicated by blue line and surface in Fig. 2(e) and 2(f)). In the following, we will use the schematic contours of the k_F positions, indicated by green surfaces in Fig. 2(f), to describe the bulk Fermi surface.

Fig. 3(a) and 3(b) show the occupied bands, along the ΓX direction in the vicinity of the Γ point of the $x = 0.01$ and 0.05 samples. By aligning the k_F's of the ARPES data with those of the LDA dispersions[11], we estimate the dopings of the $x = 0.01$ and $x = 0.05$ samples to be slightly higher than the nominal dopings (1.5±0.2% and 5.6±0.5 %, respectively: Fig. 3(e)), likely due to a small oxygen deficiency at the surface.

Having isolated the occupied part of the conduction bands (Fig. 3(a)-3(d)), let us now turn to the interpretation of the data. In the data one can discern a weak kink in the dispersion at approximately 20 meV binding energy (blue arrows, Fig. 3(a) and 3(b)). This is more clear in the $x = 0.01$ sample, since in the x=0.05 sample it resides in a region where the dispersion has a strong curvature (Fig. 3(e)). Such a weak kink structure in the dispersion indicates a perturbative coupling with a bosonic mode at this energy. This interpretation is supported by the observation that the intensity rapidly increases below the kink energy; above the kink energy, an extra decay channel opens up that will smear the QP peak. To quantify the coupling to this boson, we extracted the band velocities for the $x = 0.01$ case at binding energies below (v_{lo}) and above (v_{hi}) the kink energy (see Fig. 3(f)) to be ∼0.16 eV$\mathring{A}$ and 0.21 eV$\mathring{A}$, respectively. The mass renormalization is therefore $v_{hi}/v_{lo} = m^*/m$ ∼1.3, indicating a coupling to this particular boson $\lambda' \equiv m^*/m - 1 = 0.3$.

Given that the signals are rather smeared at higher energies we cannot exclude the presence of other kinks associated with higher energy modes. However, the data permit us to track the overall width of the occupied parts of the conduction bands. For the $x = 0.01$ sample we find the band bottom at ∼58 meV whereas the LDA calculation indicates it to be at ∼97 meV [11] (Fig. 3(e)). It follows that the overall width of the occupied band is renormalized by a factor of ∼1.7 (W_{LDA}/W_{exp}). The total mass renormalization is the product of the bandwidth and kink renormalization factors and we find this to be $1.7 \times 1.3 \simeq 2.2$ in the $x = 0.01$ sample, close to the estimate 2-3 deduced from the optical measurements[11].

To compare with STO data, Fig. 4 shows ARPES data of $La_{1-x}Sr_xCuO_4$ with x=0.01, as a lightly doped Mott insulator. The momentum is along the (0,0) to (π, π)

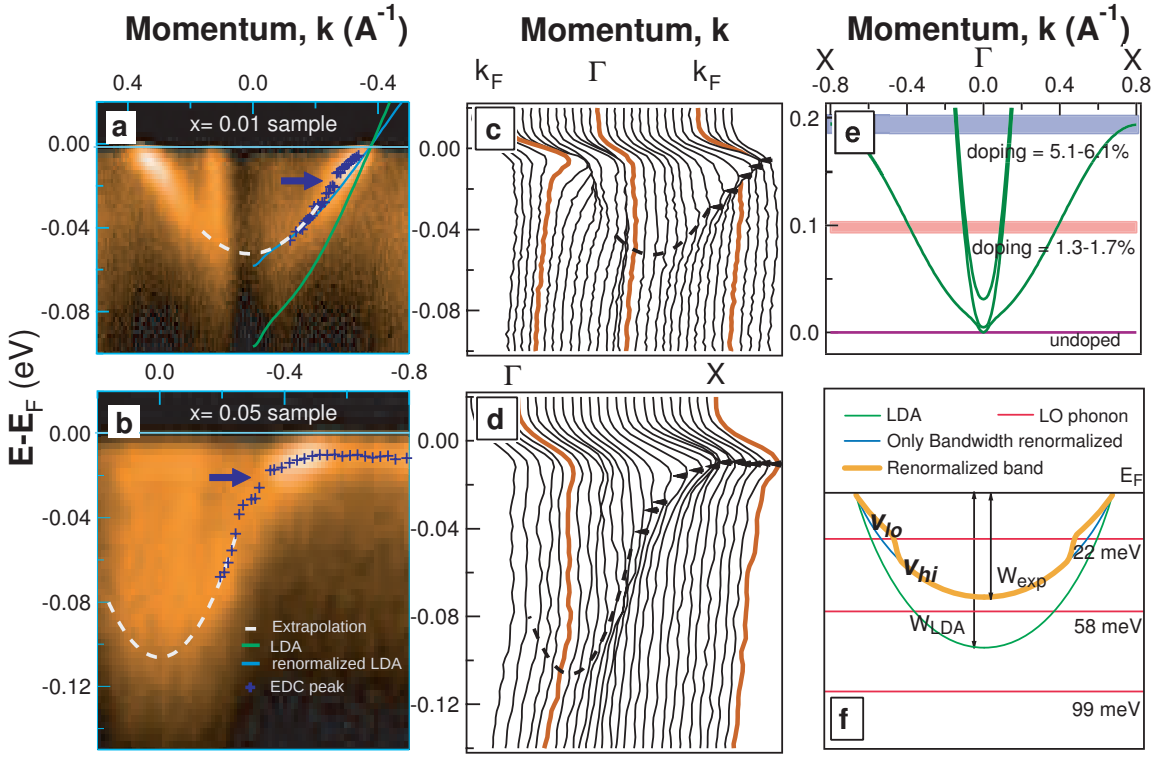

Figure 3. ((a), (b) Quasi-particle band dispersions of x=0.01 and 0.05 samples. Cross symbols indicate peaks from energy distribution curves (EDC) and dashed lines are extrapolated to get the band bottom. The most prominent kink energy is indicated by arrows around $\sim 20meV$ for both doped samples. Possibly, there is a second kink in the x=0.05 sample between 40-60 meV but the complication from the side band makes it less clear. Note that k_z varies slightly along the k-axis of (a) and (b) (see Fig. 2). However, this change has only a minute influence on the measured group velocities and will be neglected for the discussion of the mass renormalization. (c) and (d) show EDCs of ARPES data shown in (a) and (b) respectively where the EDC peak positions are marked by triangle symbols and the dash lines are extrapolations. (e) LDA band dispersion of undoped $SrTiO_3$ along ΓX[11]. Fermi levels positions for dopings = 1.3-1.7% and 5.1-6.1% are indicated by shaded areas. (f) Schematic plot of renormalized band dispersion in the forms of "kink" and reduced bandwidth caused by phonons whose mode energies are lower and higher than the electron bandwidth, respectively.

direction. We note that the data in Fig. 4 is already subtracted by the non-dispersive background of oxygen valance band. In contrast to STO, the spectrum (see red line in Fig. 4(b)) shows a small quasi-particle peak with large Frank-Condon type broad hump around 400 meV - a signature of small polaron formation. LSCO data also shows a clear kink in the dispersion, indicating a strong electron-phonon coupling at around 70 meV (see arrow in Fig. 4(a)); to quantify this coupling, we extracted the band velocities at binding energies below (v_{lo}) and above (v_{hi}) the kink energy to be $\sim$1.66 eV$\AA$ and 6.14 eV$\AA$, respectively. Therefore, the mass renormalization factor from this kink feature is $v_{hi}/v_{lo} = m^*/m \sim 3.7$. A use of $\lambda' \equiv m^*/m - 1$ would give λ' of 2.7, giving a clear

contrast to the extracted value of ∼0.3 from the kink feature of the x=0.01 STO sample.

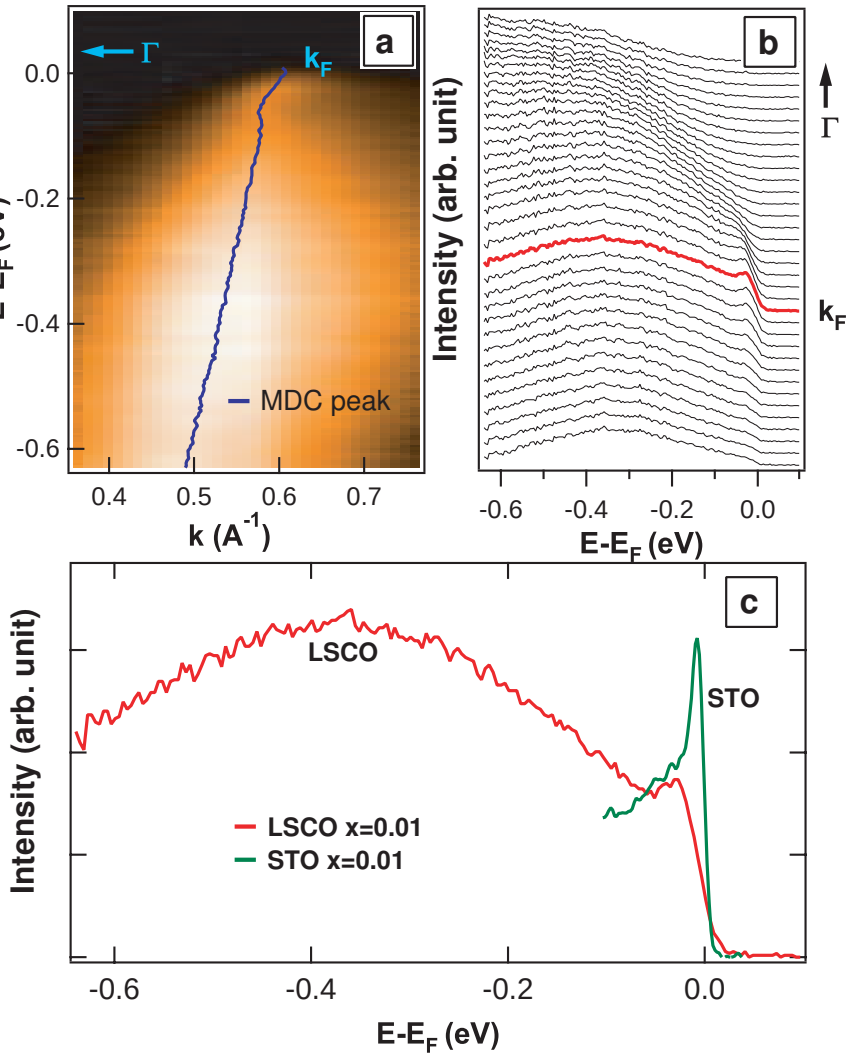

Figure 4. ARPES data of $La_{1-x}Sr_xCuO_4$ with x=0.01. (a) shows the raw ARPES data and blue line indicates the peak position in momentum distribution curves (MDC) where the big arrow indicates the kink in dispersion at binding energy ∼70meV. (b) shows the corresponding energy distribution curves. (c) Comparison of ARPES spectra at k_F of 1) x=0.01 STO sample along $\Gamma - X$ direction and 2) 1% doping $La_{2-x}Sr_xCuO_4$ along (0,0) to (π, π) direction.

4. Discussion and Conclusion

How to interpret these findings from STO data? The 20 meV kink is certainly related to a phonon. A-priori one can be less certain about the cause of overall bandwidth renormalization because an electronic origin cannot be excluded. However, although LDA is well known to underestimate band gaps in band-insulators, it does not usually underestimate the bandwidths and our extracted renormalization factor may be regarded

as an upper value. At the same time, the phonon dispersions of STO have been measured by infrared and Raman spectroscopy[15] and neutron scattering[17, 18, 19, 20] in great detail; the phonon modes are in the range of 0-100 meV where much of the phonon spectrum extends to energies that are larger than the Fermi energy of at least the $x = 0.01$ system. Under such an anti-adiabatic condition, one expects the electron-phonon coupling to give rise to an overall bandwidth renormalization that can be estimated from the mass-renormalization formulae for the isolated polaron [1]. Since the focus here is on the surprisingly moderate el-ph coupling, we attribute all the renormalization to el-ph interaction which sets the upper bound for the value of $\lambda \sim 1$. An overall coupling $\lambda \sim 1$ can mean both that small, self-trapped polarons are formed but also that the system stays itinerant. What decides the nomenclature is the length scale of the relevant electron-phonon couplings.

When the el-ph coupling is short ranged, small polarons are expected. One can take the cuprates as an example where an effective $\lambda \simeq 1$ corrected for electronic band narrowing effects [21] that enhance the impact of el-ph interaction is believed to be responsible for the multi-phonon Franck-Condon peak indicated in Fig. 4(c). Here we should note that m* is no longer linear with λ and increases rapidly near the small-to-large polaron crossover around $\lambda \simeq 1$. For $\lambda \simeq 1$ in cuprates (e.g. in the case of LSCO shown in Fig. 4), the actual face value of mass renormalization could be as large as 3.7; hence, λ' defined by $m^*/m - 1$ would be 2.7.

The most striking aspect of the STO data is that such effects due to small-polaron formation are entirely absent in STO, where instead the electrons remain strongly coherent as manifested by the strong energy-momentum dispersion and the rather sharp QP peaks with large pole strengths even for 1% doped sample (Fig. 4(c)). This can be reconciled with the relatively large λ assuming that the dominating electron-phonon couplings are of the long ranged, polar kind [22]. This claim can in fact be further substantiated by the finding that our data are in semi-quantitative agreement with 'naive' continuum limit estimations of the polar el-ph interactions[23, 10]. In this way only the long ranged electrostatic interactions are taken into account with the longitudinal optical (LO) phonons, omitting completely short range interactions involving the transversal optical (TO) phonons that are in reality always present.

Starting from this perspective, let us first discuss why the large bulk dielectric constant is actually of little relevance to the issue of polaron formation. The dielectric constants at zero frequency (ε_0) and at frequencies large compared to the phonon energy (ε_∞) are related to the frequencies of LO and TO phonons as $\varepsilon_0/\varepsilon_\infty = \Pi_a(\omega_{aLO}/\omega_{aTO})^2$ where a specifies the phonon branch. A large ε_0 signals a softening of the TO phonon that eventually can condense in a ferroelectric state. The Fröhlich polar el-ph interactions involve the LO phonons and these are therefore not communicating with the large ε_0. Another issue is that the short-range coupling to this TO phonon could be enhanced due to the softening of the frequency ω_{TO}. However, since the softening occurs only in a narrow region in momentum space characterized by the scale $a/\xi \cong 0.1$ (ξ: correlation length) [18, 19], the increase in the coupling constant $\Delta\lambda$ of the order of

$\Delta\lambda \cong \lambda(\omega_{TO}^0/\omega_{TO})^2(a/\xi)^3$ is small.

Table 1. Comparison of features between $SrTiO_3$ and cuprates - perovskite band and Mott insulators.

Feature	Mott Insulator (La_2CuO_4)	Band Insulator ($SrTiO_3$)
Mass renormalization factor from kink feature at small doping x=0.01	∼3.7	∼1.3
Small polaronic effect at small doping	Yes	No
Large pseudogap behavior at small doping	Yes	No
Small Fermi Surface pocket at small doping	Maybe(YBCO)[25]	Yes
Dielectric constant (undoped)	~ 20[26]	$\sim 10^2 - 10^4$

Under these assumptions one is, according to the calculations of Devreese et al.[23, 10], left with three LO phonons at (for $q = 0$) 22, 58, and 99 meV with coupling constants α_i of 0.018, 0.945 and 3.090, respectively. Using that, for weak coupling, $\lambda_i = \alpha_i/6$ [1, 24] this translates into λ_i's of 0.003, 0.16 and 0.6 respectively. These modes are indicated together with the electronic dispersions in the schematic Fig. 3(f). The low energy kink in the electron dispersions matches very well with the 22 meV mode associated with Sr-O bond stretching [20]. The other two phonon modes are at higher energy than the band bottom and hence they should cause an overall band width reduction. From the calculation, the coupling constants α of these 58-meV and 99-meV modes will give a bandwidth-renormalized factor of 1.76, i.e. very close to our extracted value of ∼1.7. The polar el-ph calculation strongly underestimates the $\lambda' \simeq 0.3$ coupling to the 22 meV phonon. The main coupling from this Sr-O bond stretching modes comes from large momenta near the zone boundary as in the cuprates and is expected from general grounds due to the displacement eigenvectors. Thus, it is a local deformation. As we discussed in the previous paragraph this could well be significantly enhanced by the proximity to the ferroelectric transition, a reason why its main impact is only on the low energy phonon. However, given that the coupling is still moderate and this phonon is of the adiabatic/Eliashberg kind, it does not interfere with the consistency of our argument.

While small polarons are absent in STO, the cuprates at similar doping show a sharp contrast in displaying strong el-ph coupling with mass renormalization as large as 3.7 (see Table 1 for the comparison between LSCO and $SrTiO_3$). For the following reasons, the carriers doped into a Mott insulator can be subject to a stronger short-range

el-ph interaction. One is that the additional polaronic effect due to the magnetic degrees of freedom enhances the effective mass, and hence collaborate to form the composite small polaron with magnon and phonon clouds[27]. Another reason is that fluctuations with large momentum (e.g. k=$(\pi/2, \pi/2)$ of the antiferromagnetic state in the cuprates) are involved in dressing the doped carriers. Starting from the Fröhlich interaction, the exchange of this large momentum can lead to the short-range el-ph interaction. In the case of a band insulator, the large momentum in this same order of magnitude is not immediately available. Therefore, small polaron formation is more likely to occur in a Mott insulator than in a band insulator.

In conclusion, we have shown the quite unexpected results that there is little evidence for small polaron formation in lightly doped $SrTiO_3$ indicating that the large dielectric behavior can occur independently of strong el-ph interactions. In turn, this indicates that in doped Mott insulators like the cuprates, the dressing of electrons by spin excitations and strong correlations conspire to give a short-range el-ph interaction able to trap doped carriers and more readily form polarons.

5. Acknowledgments

We gratefully thank I.I. Mazin for providing the unpublished LDA calculations and H. Takagi and J. Matsuno for crystal information. This work is supported by the Department of Energy, Office of Basic Energy Sciences under contract DE-AC02-76SF00515. C.C.C. is supported in part by National Science Council, Taiwan, under Grant No. NSC-095-SAF-I-564-013-TMS.

References

[1] Devreese JT and Alexandrov AS 2009 *Rep Prog Phys* **72** 066501
[2] Alexandrov AS and Mott NF (1994) *Rep Prog Phys* **57** 1197
[3] Shen KM, *et al.* 2004 *Phys Rev Lett* **93** 267002
[4] Yoshida T, *et al.* 2003 *Phys Rev Lett* **91** 027001
[5] Mannella N, *et al.* 2005 *Nature* **438** 474
[6] Muller KA and Burkard H 1979 *Phys Rev B* **19** 3593
[7] Koonce CS, *et al.* 1967 *Phys Rev* **163** 380
[8] Suzuki H, *et al.* 1996 *J Phys Soc Jpn* **65** 1529
[9] Bednorz JG and Muller KA 1988 *Rev Mod Phys* **60** 585
[10] Verbist G, Peeters FM and Devreese JT 1992*Ferroelectrics* **130** 27
[11] Van Mechelen JLM, *et al.* 2008 *Phys Rev Lett* **100** 226403
[12] Imada M, Fujimori A and Tokura Y 1998 *Rev Mod Phys* **70** 1039
[13] Ishida Y, *et al.* 2008 *Phys Rev Lett* **100** 056401
[14] Aiura Y, *et al.* 2002 *Surf Sci* **515** 61
[15] Cardona M 1965 *Phys Rev* **140** A651
[16] Luo W, *et al.* 2004 *Phys Rev B* **70** 214109
[17] Cowley RA 1964 *Phys Rev* **134** A981
[18] Shirane G and Yamada Y 1969 *Phys Rev* **177** 858
[19] Shirane G 1974 *Rev Mod Phys* **46** 437
[20] Choudhury N, *et al.* 2008 *Phys Rev B* **77** 134111

[21] Rosch O, *et al.* 2005 *Phys Rev Lett* **95** 227002
[22] Toyozawa Y 2003 *Optical Processes in Solids* (Cambridge University Press, Cambridge), pp 149-187.
[23] Eagles DM 1965 *J Phys Chem Solids* **26** 672
[24] Feynman RP 1955 *Phys Rev* **97** 660
[25] Doiron-Leyraud N, *et al.* 2007 *Nature* **447** 565
[26] Tamasaku K, *et al.* 1992 *Phys Rev Lett* **69** 1455
[27] Mishchenko AS and Nagaosa N 2004 *Phys Rev Lett* **93** 036402